The Dimensional Synthesis of Planar Parallel Cable-Driven Mechanisms Through Convex Relaxations

K. Azizian
e-mail: kaveh.azizian.1@ulaval.ca

P. Cardou
e-mail: pcardou@gmc.ulaval.ca

Département de Génie Mécanique,
Université Laval,
Québec, QC, G1V 0A6, Canada

The wrench-closure workspace (WCW) of parallel cable-driven mechanisms is the set of poses for which any wrench can be produced at the end-effector by a set of positive cable tensions. In this paper, we tackle the dimensional synthesis problem, namely, that of finding a geometry for a planar parallel cable-driven mechanism (PPCDM) whose WCW contains a prescribed workspace. To this end, we first recall a linear program to determine whether a given pose is inside or outside the WCW of a given PPCDM. The relaxation of this linear program over a box leads to a nonlinear feasibility problem that can only be satisfied when this box is completely inside the WCW. We extend this feasibility problem to find a PPCDM geometry whose WCW includes a given set of boxes. These boxes represent the prescribed workspace or an estimate thereof, which may be obtained through interval analysis. Finally, we introduce a nonlinear program through which the PPCDM geometry is changed while maximizing the scaling factor of the prescribed set of boxes. When the optimum scaling factor is greater or equal to one, the WCW of the resulting PPCDM contains the set of boxes. [DOI: 10.1115/1.4006952]

Keywords: wrench-closure workspace, cable-driven mechanism, linear programming, dual problem, nonlinear programming, convex relaxation, dimensional synthesis, interval analysis

1 Introduction

A PPCDM generally consists of a moving platform (MP) and a fixed frame, which are connected with multiple cables, as shown in Fig. 1. Each cable is wound around an actuated reel fixed to the base, and is attached to the moving platform at its other end. The cables and the moving platform are assumed to be contained in the same plane. The actuated reels control the position and orientation of the moving platform in this plane by controlling the lengths of their corresponding cables.

Generally speaking, cable-driven robots have several advantages as are described in Ref. [1], including remote location of motors and controls, rapid deployability, high load capacity, reliability, and *potentially large workspaces*. Because of these characteristics, these robots are ideal for many tasks, such as handling of hazardous materials and disaster search and rescue efforts [2]. Additionally, cable-driven robots such as the SkyCam [3] have found success in the fields of sports and entertainment. Recently, these robots have demonstrated their capabilities for actuated sensing [4] and [5] aquatic applications as well. Although many applications involve spatial cable-driven robots, however, there is also an interest for planar cable-driven robots in several applications [5–7].

Since the cables can be wound onto reels over long lengths, the workspace of a cable-driven mechanism can be larger than that of a conventional parallel mechanism. This is only a potential advantage, however, as the workspace of a PPCDM is further limited by the inability of cables to push on the moving platform. Indeed, there are many poses inside this workspace for which the cables cannot balance all applied wrenches, because at least one of them would have to push on the platform. More formally, the WCW is the set of poses for which all applied wrenches are feasible. An applied wrench is said to be feasible if it can be balanced by a set of non-negative cable tensions. This is a special case of the wrench-feasible workspace (WFW), which is the set of poses of the moving platform for which the cables can balance any wrench of a given set of wrenches, such that the tension in each cable remains within a prescribed range.

The WCW of cable-driven parallel mechanisms has been studied in several research works. A necessary condition for the WCW to be nonempty is that the number of cables be greater than the number of degrees of freedom of the moving platform [8,9]. We refer to these mechanisms as fully constrained, as opposed to

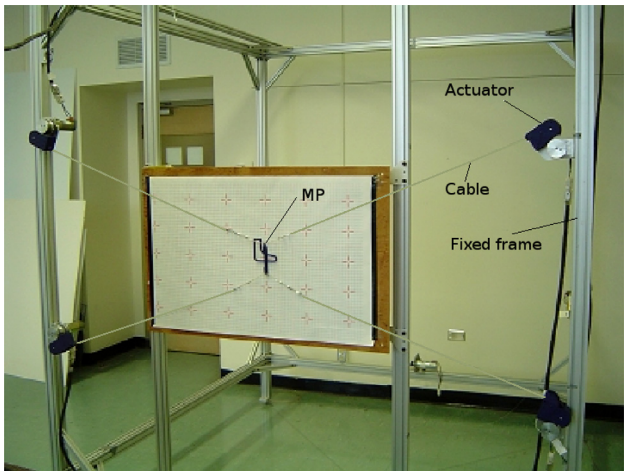

Fig. 1 A prototype of planar parallel cable-driven mechanism with four cables at Robotics Laboratory of Université Laval [6]

Contributed by the Mechanisms and Robotics Committee of ASME for publication in the JOURNAL OF MECHANISMS AND ROBOTICS. Manuscript received October 14, 2011; final manuscript received May 11, 2012; published online June 29, 2012. Assoc. Editor: Vijay Kumar.

under constrained cable-driven mechanisms, which use the weight of the platform to put certain tension on some cables [10]. For fully constrained cable-driven mechanisms, the WCW depends only on the geometry of the mechanism, i.e, on the locations of the attachment points on the fixed frame and on the moving platform.

A large body of literature is already available for determining the workspace of parallel cable-driven robots due to the unilateral nature of the forces applied by the cables on the mobile platform. Most of the proposed methods allow to determine the workspace of these robots, for instance, by means of a discretization method [11] or by a symbolic method [12]. Fattah and Agrawal [13] proposed a methodology to calculate the workspace of redundant and nonredundant planar cable-driven robots by means of a discretization method. In their method, tensions in the cables are calculated and conditions are obtained to verify whether a reference point on the moving platform is reachable with positive tensions. Riechel and Ebert-Uphoff [14] present a means of analytically deriving the WFW for the case of a point-mass end-effector and analyze the characteristics and trends of the WFW. Some authors apply the antipodal theorem to calculate the WCW of PPCDMs [15]. All these works pertain to the analysis of the workspace of cable-driven parallel mechanisms. Very few of them tackle the difficult design problem of finding a parallel cable-driven mechanism from a prescribed workspace, i.e., the synthesis problem.

Gouttefarde et al. [16] propose an interval-analysis-based approach to find boxes guaranteed to be fully inside or fully outside of the WFW. The proposed approach can be applied to verify whether a given prescribed workspace is fully included in the WFW of a given cable-driven mechanism. They also show that their proposed method can deal with small uncertainties on the geometric design parameters of a parallel cable robot. This is a valuable tool for the dimensional synthesis of cable-driven robots, but because of its computational cost, we do not know that it has been already applied to such problems. Besides, by their numerical nature, interval arithmetics cannot provide symbolic conditions that constrain the design parameters within a feasible set, as is done in this paper.

To the knowledge of the authors, Hay and Snyman [17] were the first and only researchers to report directly on the synthesis of parallel cable-driven manipulators. They defined the dexterous workspace of a PPCDM as the intersection of all constant orientation workspaces in a given set of rotation angles, while cable tensions are constrained to lie within a given set and cable lengths are greater than a given minimum. Their main goal is to maximize the area of the dexterous workspace for a given range of rotation angles by finding the locations of fixed points of the robot along a fixed rectangular frame. They begin with a randomly chosen PPCDM design and maximize the area of its dexterous workspace by varying its geometry. In this manner, they find a locally optimum configuration of the fixed points of the robot, while the locations of the attachment points on the platform have already been assumed. Therefore, this locally optimum robot design corresponds to a dexterous workspace of maximum area, but not for a *prescribed workspace*.

In this paper, we seek to obtain the geometry of a PPCDM for a prescribed workspace. The main goal of this paper is to devise a method for the dimensional synthesis of planar parallel cable-driven mechanisms. In order to achieve this goal, we first recall the kinetostatic model of a fully constrained PPCDM and formally define its WCW in Sec. 2. In Sec. 3, we introduce a linear program (LP) to verify whether a given pose is inside or outside of the WCW of a PPCDM. In Sec. 4, we modify this linear program to obtain a sufficient condition for a given box to lie inside the WCW. We do this through convex relaxations, a technique that has become popular in some fields of applied science [18,19] but has received less attention from the robotics community. Porta et al. [20] are the only researchers who have used this technique for the analysis of robots, to the best of our knowledge. The developed linear program is then turned into a nonlinear nonconvex feasibility problem representing the dimensional synthesis of PPCDMs in Sec. 5. In the same section, this feasibility problem is turned into a nonlinear program by introducing a scaling factor of the prescribed workspace as the objective function to be maximized. We illustrate the proposed formulations with synthesis examples throughout Sec. 5.

2 Kinetostatic Model

Before searching for the geometry of a PPCDM for a prescribed WCW, we have to set up a precise mathematical description of the geometry of such a robot, and of its wrench-closure workspace. Such a PPCDM is schematically shown in Fig. 2. It consists of an MP that is connected by m cables to m fixed points A_i, $i = 1, \ldots, m$. Cable i is attached to the MP at B_i, and winds at A_i around an actuated reel.

In order to analyze the motion of the MP, we have to consider two frames: the reference frame $\mathcal{A}$, which is fixed to the base, and the moving frame $\mathcal{B}$, which is attached to a reference point of the MP. We use the following notation for the analysis of a generic PPCDM:

- Vector $\mathbf{a}_i \in \mathbb{R}^2$ represents the position of the actuated reel A_i in the fixed frame $\mathcal{A}$.
- Vector $\mathbf{b}_i \in \mathbb{R}^2$ is a constant vector and represents the position of the attachment point B_i of the ith cable in frame $\mathcal{B}$.
- Vector $\mathbf{p} \in \mathbb{R}^2$, which is expressed in $\mathcal{A}$, represents the position of the point P with respect to point O.
- Vector $\mathbf{c}_i$ points from B_i to A_i, and its norm represents the length of the ith cable.
- ϕ is the angle between the fixed axis X and the moving axis X'.

Vector $\mathbf{c}_i$ representing the ith cable is obtained as

$$\mathbf{c}_i = \mathbf{a}_i - \mathbf{p} - \mathbf{Q}\mathbf{b}_i \tag{1}$$

where $\mathbf{Q}$ is the rotation matrix taking the fixed frame onto the moving frame and can be expressed as

$$\mathbf{Q} = \mathbf{1}_{2\times 2}\cos\phi + \mathbf{E}\sin\phi \tag{2}$$

where, $\mathbf{E} = \begin{bmatrix} 0 & -1 \\ 1 & 0 \end{bmatrix}$ and $\mathbf{1}_{2\times 2} \in \mathbb{R}^{2\times 2}$ is the 2×2 identity matrix. The wrench applied at P, the origin of the moving frame, by the ith cable is

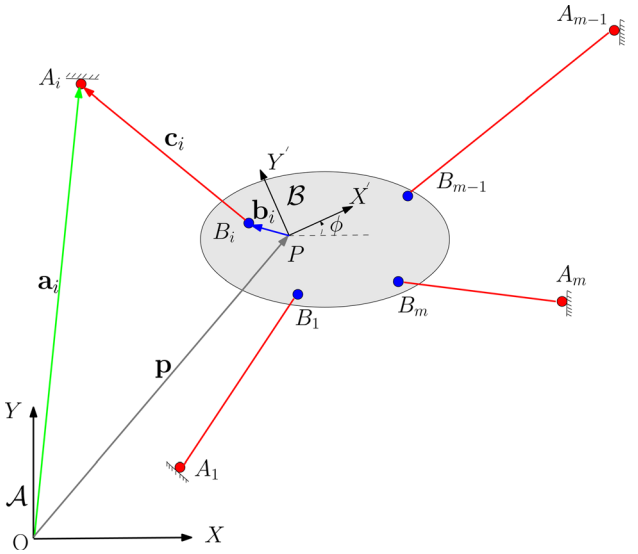

Fig. 2 Sketch of an *m*-cable PPCDM

$$\mathbf{v}_i = [\mathbf{f}_i^T \quad n_i]^T = \left[\frac{t_i}{l_i}\mathbf{c}_i^T \quad \det\left(\mathbf{Q}\mathbf{b}_i \ \frac{t_i}{l_i}\mathbf{c}_i\right)\right]^T \tag{3}$$

where $\mathbf{f}_i$ and n_i are, respectively, the force and moment about P produced by the ith cable, and l_i and t_i are the length and tension of the same cable, respectively. If we assume that points A_i and B_i do not coincide, then the wrench applied to the platform by cable i is $\frac{t_i}{l_i}\mathbf{w}_i$, with $\mathbf{w}_i$ defined as $\mathbf{w}_i = \begin{bmatrix}\mathbf{c}_i^T & \mathbf{c}_i^T & \mathbf{EQb}_i\end{bmatrix}^T$.

This definition shows that w_i is a function of the geometric parameters of the mechanism and the orientation angle of the MP. We define the wrench matrix and tension vector of the mechanism as $\mathbf{W} = [\mathbf{w}_1 \quad \mathbf{w}_2 \quad \cdots \quad \mathbf{w}_m]$ and $\mathbf{t} = \begin{bmatrix}\frac{t_1}{l_1} & \frac{t_2}{l_2} & \cdots & \frac{t_m}{l_m}\end{bmatrix}^T$, respectively. Upon substituting Eq. (1) into the expression for $\mathbf{w}_i$, we obtain

$$\mathbf{w}_i = \begin{bmatrix}\mathbf{a}_i - \mathbf{p} - \mathbf{Q}\mathbf{b}_i \\ (\mathbf{a}_i - \mathbf{p} - \mathbf{Q}\mathbf{b}_i)^T\mathbf{EQb}_i\end{bmatrix} = \begin{bmatrix}\mathbf{a}_i - \mathbf{p} - \mathbf{Q}\mathbf{b}_i \\ \mathbf{a}_i^T\mathbf{EQb}_i - \mathbf{p}^T\mathbf{EQb}_i\end{bmatrix}$$

Because $\mathbf{w}_i$, $i = 1, \ldots, m$, are the columns of the wrench matrix $\mathbf{W}$, we can rewrite this matrix in the compact form

$$\mathbf{W} = \begin{bmatrix}\mathbf{A} - \mathbf{p}\mathbf{1}_m^T - \mathbf{QB} \\ \mathbf{f}^T - \mathbf{p}^T\mathbf{EQB}\end{bmatrix} \tag{4}$$

where

$$\mathbf{A} \equiv [\mathbf{a}_1 \quad \cdots \quad \mathbf{a}_m] \in \mathbb{R}^{2\times m}, \quad \mathbf{B} \equiv [\mathbf{b}_1 \quad \cdots \quad \mathbf{b}_m] \in \mathbb{R}^{2\times m}$$
$$\mathbf{f} \equiv \begin{bmatrix}\mathbf{b}_1^T\mathbf{Q}^T\mathbf{E}^T\mathbf{a}_1 & \cdots & \mathbf{b}_m^T\mathbf{Q}^T\mathbf{E}^T\mathbf{a}_m\end{bmatrix}^T \in \mathbb{R}^m \tag{5}$$

For the purposes of this work, we must explicit the relationship between $\mathbf{W}$ and ϕ. Therefore, we substitute Eq. (2) in Eq. (5) which leads to

$$\mathbf{f} = \cos\phi\mathbf{u} + \sin\phi\mathbf{v} \tag{6}$$

where $\mathbf{u} \equiv \begin{bmatrix}\mathbf{b}_1^T\mathbf{E}^T\mathbf{a}_1 \cdots \mathbf{b}_m^T\mathbf{E}^T\mathbf{a}_m\end{bmatrix}^T \in \mathbb{R}^m$ and $\mathbf{v} \equiv -\begin{bmatrix}\mathbf{b}_1^T\mathbf{a}_1 \cdots \mathbf{b}_m^T\mathbf{a}_m\end{bmatrix}^T \in \mathbb{R}^m$, and, consequently, the wrench matrix can be rewritten as

$$\mathbf{W} = \mathbf{W}_0 + \mathbf{W}_1\cos\phi + \mathbf{W}_2\sin\phi \tag{7}$$

where $\mathbf{W}_0 = \begin{bmatrix}\mathbf{A}^T - \mathbf{1}_m\mathbf{p}^T & \mathbf{0}_m\end{bmatrix}^T \in \mathbb{R}^{3\times m}$, $\mathbf{W}_1 = \begin{bmatrix}-\mathbf{B}^T & \mathbf{u}\end{bmatrix}^T \in \mathbb{R}^{3\times m}$, and $\mathbf{W}_2 = \begin{bmatrix}-\mathbf{B}^T\mathbf{E}^T & \mathbf{v} + \mathbf{B}^T\mathbf{E}^T\mathbf{p}\end{bmatrix}^T \in \mathbb{R}^{3\times m}$. Then, the static equilibrium of the moving platform may be expressed as

$$\mathbf{W}\mathbf{t} + \mathbf{w}_P = \mathbf{0}_3 \tag{8}$$

where $\mathbf{0}_3$ is the three-dimensional zero vector and $\mathbf{w}_P$ is the wrench applied on the MP at P and is equivalent to the system of external forces and moments. These external loads may include gravity forces, for example. We can now define the WCW of PPCDMs as follows.

Definition 1. *The WCW.*

The WCW of planar parallel cable-driven mechanisms is formally defined as the set of poses for which

$$\forall\mathbf{w}_P \in \mathbb{R}^3, \quad \exists\mathbf{t} \in \mathbb{R}^m | \mathbf{t} \succeq \mathbf{0}_m \quad \text{and} \quad \mathbf{W}\mathbf{t} + \mathbf{w}_P = \mathbf{0}_3$$

where the symbol $\succeq$ denotes the component wise inequality. In other words, this workspace is the set of PPCDM MP poses for which any external load applied to the MP can be balanced by a set of non-negative cable tensions.

3 Verifying Whether a Pose Lies in the WCW of a PPCDM

We restate the Theorem 1 introduced in Ref. [21] in order to determine whether a given pose is inside the WCW of the mechanism.

Theorem 1. *Primal WCW membership condition* [21].

If there is a left null vector of wrench matrix $\mathbf{W}$ *with strictly positive components, then the robot can achieve static equilibrium.*

In other words, a given pose is inside the WCW of a PPCDM if and only if there exists a set cable tensions such that

$$\mathbf{W}\mathbf{t} = \mathbf{0}_3, \mathbf{t} \succ \mathbf{0}_m \tag{9}$$

According to Theorem 1, the WCW of a PPCDM can be computed by solving the feasibility problem (9) for each pose of the MP. Therefore, the WCW of a PPCDM is the set of poses for which Eq. (9) is satisfied. We may as well use Stiemke's theorem [22] to verify whether a given pose is inside or outside the WCW. We recall this theorem as follows.

Theorem 2 (Stiemke's Theorem). *Dual WCW membership condition* [12].

A pose is outside the WCW of a PPCDM if and only if there exists a small-displacement screw $\lambda \in \mathbb{R}^3$ *such that*

$$\begin{aligned}\mathbf{W}^T\lambda &\succeq \mathbf{0}_m \\ \mathbf{W}^T\lambda &\neq \mathbf{0}_m\end{aligned} \tag{10}$$

We can now introduce the following feasibility problem to calculate the WCW of a PPCDM:

$$\begin{aligned}\mathbf{W}^T\lambda &\succeq \mathbf{0}_m \\ \mathbf{1}_m^T\mathbf{W}^T\lambda &= 1\end{aligned} \tag{11}$$

where $\mathbf{1}_m = [1 \quad 1 \quad \cdots \quad 1]^T \in \mathbb{R}^m$. This problem yields a feasible solution whenever the given pose is outside of the corresponding WCW and is infeasible otherwise. In other words, the given pose is outside of the WCW if the problem admits a feasible solution and inside if it does not. Hence, this equation can be used to estimate the WCW of a given PPCDM by discretizing the examined region. This linear feasibility problem is to serve as the corner stone of the proposed formulation of the dimensional synthesis of PPCDMs.

4 Verifying Whether a Box Lies Inside the WCW

The formulations developed in the previous sections provide us with the proper tools to address our main concern: the dimensional synthesis of PPCDMs. We wish to determine whether a given small box lies completely inside the WCW of a given PPCDM for a given range of orientation angles. To this end, notice that the problem (11) can be turned into a phase-one problem as in the following Lemma.

Lemma 1. *Linear program WCW membership condition.*

Consider the linear program

$$\begin{aligned}\delta^* = \text{maximize} \quad & \delta \\ \text{subject to} \quad & \mathbf{W}^T\lambda \succeq \mathbf{0}_m \\ & \mathbf{1}_m^T\mathbf{W}^T\lambda \geq \delta \\ \text{over} \quad & \lambda \text{ and } \delta.\end{aligned} \tag{12}$$

Then, we have

$$\delta^* = \begin{cases}+\infty & \text{if the pose lies outside the WCW} \\ 0 & \text{otherwise}\end{cases} \tag{13}$$

Proof. First, consider the case where the MP pose lies outside the WCW. From Eq. (11), we then have a λ such that $\mathbf{W}^T\lambda \succeq 0_m$ and $\mathbf{1}_m^T\mathbf{W}^T\lambda = 1$. Thus, the point $(\lambda, \delta) = (\lambda, 1)$ lies in the feasible set of problem (12), and so do the points $(k\lambda, k)$, where $k \geq 0$. In this latter case, the objective to be maximized, k, can be chosen arbitrarily large, so that the optimization problem (12) becomes unbounded.

Second, we treat the case where the MP pose lies inside the WCW. Then, from Theorem 2, there exists no λ such that $\mathbf{W}^T\lambda \succeq \mathbf{0}_m$ and $\mathbf{W}^T\lambda \neq \mathbf{0}_m$. Conversely, any $\lambda \in \mathbb{R}^3$ satisfying $\mathbf{W}^T\lambda \succeq \mathbf{0}_m$ also satisfies $\mathbf{W}^T\lambda = \mathbf{0}_m$. Substituting these results in Eq. (12) inevitably leads to $\delta = 0$, provided that there exists a feasible λ. Notice that $(\lambda, \delta) = (\mathbf{0}_3, 0)$ is always a feasible point of problem (12), so that its optimum is always 0 when the pose lies inside the WCW. □

Consider now a box $\mathcal{B}$ with the lower-left and upper-right corners $(\underline{\phi}, \underline{\mathbf{p}})$ and $(\bar{\phi}, \bar{\mathbf{p}})$, respectively, i.e., $\mathcal{B} = \{(\phi, \mathbf{p}) \in \mathbb{R} \times \mathbb{R}^2 : \underline{\phi} \leq \phi \leq \bar{\phi}, \underline{\mathbf{p}} \preceq \mathbf{p} \preceq \bar{\mathbf{p}}\}$. In order to find a necessary condition for $\mathcal{B}$ to be outside of the WCW, we substitute Eq. (7) in problem (12), we let p in the decision variables of the problem, while confining it to $\mathcal{B}$. This leads to

$$\begin{aligned}
&\text{maximize } \delta,\\
&\text{subject to } \mathbf{0}_m \preceq (\mathbf{A}^T - \mathbf{1}_m\mathbf{p}^T - \mathbf{B}^T\cos\phi - \mathbf{B}^T\mathbf{E}^T\sin\phi)\mu\\
&\qquad + (\mathbf{u}\cos\phi + \mathbf{v}\sin\phi - \mathbf{B}^T\mathbf{E}^T\mathbf{p}\cos\phi\\
&\qquad + \mathbf{B}^T\mathbf{p}\sin\phi)\mu_0\\
&\qquad \delta \leq \mathbf{1}_m^T((\mathbf{A}^T - \mathbf{1}_m\mathbf{p}^T - \mathbf{B}^T\cos\phi - \mathbf{B}^T\mathbf{E}^T\sin\phi)\mu\\
&\qquad\quad + (\mathbf{u}\cos\phi + \mathbf{v}\sin\phi - \mathbf{B}^T\mathbf{E}^T\mathbf{p}\cos\phi\\
&\qquad\quad + \mathbf{B}^T\mathbf{p}\sin\phi)\mu_0)\\
&\qquad \underline{\phi} \leq \phi \leq \bar{\phi}, \underline{\mathbf{p}} \preceq \mathbf{p} \preceq \bar{\mathbf{p}}
\end{aligned} \tag{14}$$

where $\lambda \equiv \begin{bmatrix}\mu^T & \mu_0\end{bmatrix}^T$.

Considering $\mathbf{p}$, the operation-point-position and ϕ, the MP orientation as optimization variables, we obtain a nonlinear optimization problem. If one were able to solve this complex problem, then it would be possible to determine whether there is at least one pose of $\mathcal{B}$ that is not inside the WCW. Conversely, if the global optimum of (14) is $\delta^\star = 0$, then box $\mathcal{B}$ is completely inside the WCW. This global optimum, however, is very difficult to compute in general. Instead, we resort to convex relaxations, where by we relax the nonconvex constrained of (14) into convex ones, over the box $\mathcal{B}$. To this end, let us consider the trilinear terms of Eq. (14), i.e., $\mathbf{p}\cos\phi\mu_0$ and $\mathbf{p}\sin\phi\mu_0$ and define the new variables

$$\alpha \equiv \mathbf{p}\cos\phi \quad \text{and} \quad \beta \equiv \mathbf{p}\sin\phi \tag{15}$$

Substituting these new variables in Eq. (14) reduces the degree of the constraints to 2, while adding four equality constraints. For the given box $\mathcal{B}$, we can obtain upper and lower bonds on these new variables α and β, as they are the multiplications of the interval variables [23] $\mathbf{p}$, $\cos\phi$, and $\sin\phi$. For a given interval of orientation angles, $\underline{\phi} \leq \phi \leq \bar{\phi}$, we have

$$\underline{c} \leq \cos\phi \leq \bar{c} \quad \text{and} \quad \underline{s} \leq \sin\phi \leq \bar{s} \tag{16}$$

so that

$$\underline{\alpha} \preceq \alpha \preceq \bar{\alpha} \quad \text{and} \quad \underline{\beta} \preceq \beta \preceq \bar{\beta} \tag{17}$$

where $\underline{\alpha} = \min(\mathbf{S}_\alpha), \bar{\alpha} = \max(\mathbf{S}_\alpha)$; $\underline{\beta} = \min(\mathbf{S}_\beta), \bar{\beta} = \max(\mathbf{S}_\beta)$; and $\mathbf{S}_\alpha = \begin{bmatrix}\underline{\mathbf{p}}\underline{c} & \underline{\mathbf{p}}\bar{c} & \bar{\mathbf{p}}\underline{c} & \bar{\mathbf{p}}\bar{c}\end{bmatrix} \in \mathbb{R}^{2\times 4}$, $\mathbf{S}_\beta = \begin{bmatrix}\underline{\mathbf{p}}\underline{s} & \underline{\mathbf{p}}\bar{s} & \bar{\mathbf{p}}\underline{s} & \bar{\mathbf{p}}\bar{s}\end{bmatrix} \in \mathbb{R}^{2\times 4}$. Let us now separate the bilinear terms appearing in Eq. (14) when considering μ, μ_0, $\mathbf{p}$, α, β, $\cos\phi$, and $\sin\phi$ as optimization variables and define the following variables:

$$\begin{aligned}
&\eta \equiv \text{diag}(\mu)\mathbf{p}, \quad \rho \equiv \mu\cos\phi, \quad \tau \equiv \mu\sin\phi, \quad \chi \equiv \alpha\mu_0,\\
&\psi \equiv \beta\mu_0, \quad \rho_0 \equiv \mu_0\cos\phi, \quad \text{and} \quad \tau_0 \equiv \mu_0\sin\phi
\end{aligned} \tag{18}$$

While the variables $\mathbf{p}$, α, β, $\cos\phi$, and $\sin\phi$ are bounded, the variables μ_0 and μ remain unbounded. For the sake of this analysis, let us assume that the signs of μ_0 and μ are known in advance and label them

$$\sigma_0 \equiv \text{sgn}(\mu_0) \quad \text{and} \quad \sigma \equiv \text{sgn}(\mu) \tag{19}$$

where sgn() represents the signum function. Knowing the signs of μ_0 and μ enables us to generate the following bounds on the newly defined variables of Eq. (18):

$$\begin{aligned}
&\text{diag}(\sigma)\text{diag}(\underline{\mathbf{p}})\mu \preceq \text{diag}(\sigma)\eta \preceq \text{diag}(\sigma)\text{diag}(\bar{\mathbf{p}})\mu\\
&\underline{c}\,\text{diag}(\sigma)\mu \preceq \text{diag}(\sigma)\rho \preceq \bar{c}\,\text{diag}(\sigma)\mu\\
&\underline{s}\,\text{diag}(\sigma)\mu \preceq \text{diag}(\sigma)\tau \preceq \bar{s}\,\text{diag}(\sigma)\mu\\
&\sigma_0\mu_0\underline{\alpha} \preceq \sigma_0\chi \preceq \sigma_0\mu_0\bar{\alpha}\\
&\sigma_0\mu_0\underline{\beta} \preceq \sigma_0\psi \preceq \sigma_0\mu_0\bar{\beta}\\
&\underline{c}\sigma_0\mu_0 \leq \sigma_0\rho_0 \leq \bar{c}\sigma_0\mu_0\\
&\underline{s}\sigma_0\mu_0 \leq \sigma_0\tau_0 \leq \bar{s}\sigma_0\mu_0
\end{aligned} \tag{20}$$

When treating σ_0 and σ as constants, the set formed by Eq. (20) represents a convex polyhedron, which approximates the nonconvex surfaces of Eq. (18). Therefore, replacing the latter with the former, we obtain a *convex relaxation* of Eq. (18). This approximation converges to the exact relationship as box $\mathcal{B}$ is shrunk to a point. This approach is called the reformulation–linearization technique, and was originally proposed by Sherali and Tuncbilek [24]. Hence, the relaxed form of problem (14) is

$$\begin{aligned}
&\text{maximize } \delta,\\
&\text{subject to } \mathbf{0}_m \preceq \mathbf{A}^T\mu - \mathbf{1}_m\mathbf{1}_2^T\eta - \mathbf{B}^T\rho - \mathbf{B}^T\mathbf{E}^T\tau + \rho_0\mathbf{u} + \tau_0\mathbf{v}\\
&\qquad - \mathbf{B}^T\mathbf{E}^T\chi + \mathbf{B}^T\psi\\
&\qquad \delta \leq \mathbf{1}_m^T\mathbf{A}^T\mu - m\mathbf{1}_2^T\eta - \mathbf{1}_m^T\mathbf{B}^T\rho - \mathbf{1}_m^T\mathbf{B}^T\mathbf{E}^T\tau\\
&\qquad\quad + \rho_0\mathbf{1}_m^T\mathbf{u} + \tau_0\mathbf{1}_m^T\mathbf{v} - \mathbf{1}_m^T\mathbf{B}^T\mathbf{E}^T\chi + \mathbf{1}_m^T\mathbf{B}^T\psi\\
&\qquad \text{diag}(\sigma)\text{diag}(\underline{\mathbf{p}})\mu \preceq \text{diag}(\sigma)\eta \preceq \text{diag}(\sigma)\text{diag}(\bar{\mathbf{p}})\mu\\
&\qquad \underline{c}\text{diag}(\sigma)\mu \preceq \text{diag}(\sigma)\rho \preceq \bar{c}\text{diag}(\sigma)\mu\\
&\qquad \underline{s}\text{diag}(\sigma)\mu \preceq \text{diag}(\sigma)\tau \preceq \bar{s}\text{diag}(\sigma)\mu\\
&\qquad\quad \sigma_0\mu_0\underline{\alpha} \preceq \sigma_0\chi \preceq \sigma_0\mu_0\bar{\alpha}\\
&\qquad\quad \sigma_0\mu_0\underline{\beta} \preceq \sigma_0\psi \preceq \sigma_0\mu_0\bar{\beta}\\
&\qquad\quad \underline{c}\sigma_0\mu_0 \leq \sigma_0\rho_0 \leq \bar{c}\sigma_0\mu_0\\
&\qquad\quad \underline{s}\sigma_0\mu_0 \leq \sigma_0\tau_0 \leq \bar{s}\sigma_0\mu_0\\
&\qquad\quad \sigma_0 = \text{sgn}(\mu_0), \sigma = \text{sgn}(\mu)
\end{aligned} \tag{21}$$

The only nonconvex constraints in problem (21) are the latter two equations, which yield exactly eight possible combinations of σ_0 and σ, namely, the solutions to

$$\sigma_0^2 = 1 \quad \text{and} \quad \text{diag}(\sigma)^2 = \mathbf{1}_{2\times 2} \tag{22}$$

Let us label these solutions $\sigma_{0,j}$ and σ_j, $j = 1, \ldots, 8$. As a result, the solution to problem (21) is the maximum of the outcomes of the eight resulting linear programs. This leads to Lemma 2.

Lemma 2. *Sufficient conditions for a box to lie inside the WCW within a given range of orientation angles.*

Consider the eight distinct linear programs

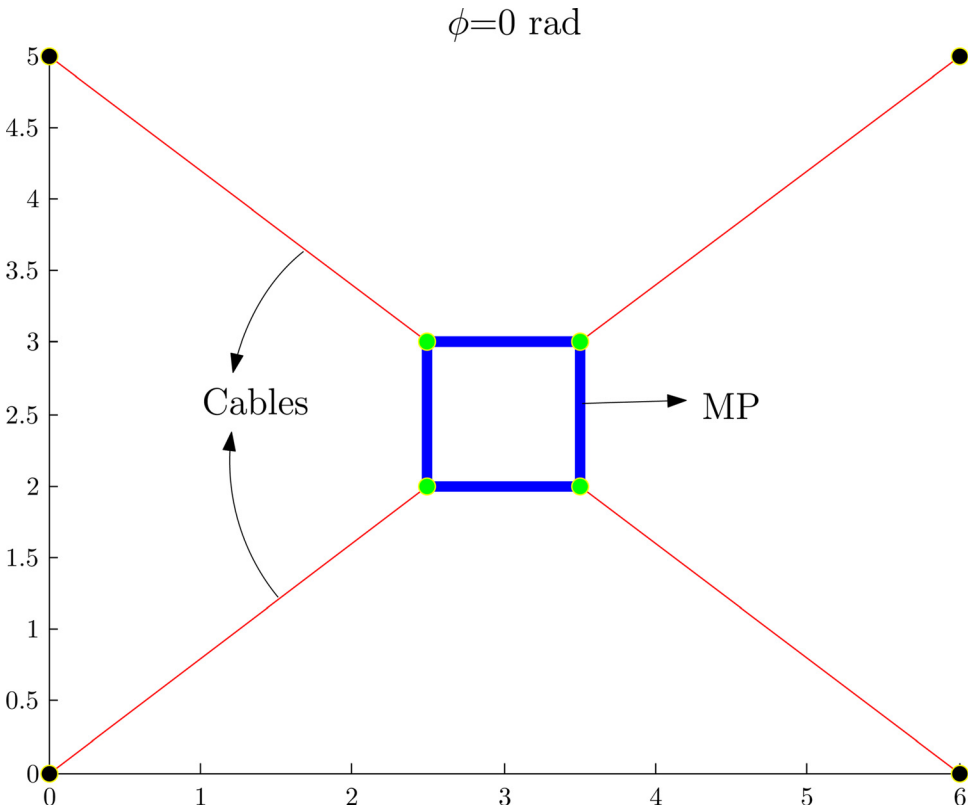

Fig. 3 A PPCDM with four cables

$$\begin{aligned} &\text{maximize} && \delta_j \\ &\text{subject to} && \mathbf{G}_j \xi_j \preceq \mathbf{0}_{m+25} \\ &&& j = 1, \ldots, 8 \end{aligned} \tag{23}$$

where $\mathbf{G}_j \equiv \begin{bmatrix} \mathbf{g}^T & 1 \\ \mathbf{R}_j^T & \mathbf{0}_{m+24} \end{bmatrix} \in \mathbb{R}^{(m+25)\times 16}$, $\mathbf{R}_j$ *and vector* $\mathbf{g}$ *are given in Appendix, and* $\xi_j = \begin{bmatrix} \mu_{0,j} & \rho_{0,j} & \tau_{0,j} & \mu_j^T & \eta_j^T & \rho_j^T & \tau_j^T & \chi_j^T & \psi_j^T & \delta_j \end{bmatrix}^T \in \mathbb{R}^{16}$. *Then, the given box* $\mathcal{B} = \{(\phi, \mathbf{p}) \in \mathbb{R} \times \mathbb{R}^2 : \underline{\phi} \leq \phi \leq \bar{\phi}, \underline{\mathbf{p}} \preceq \mathbf{p} \preceq \bar{\mathbf{p}}\}$ *is fully inside the WCW if all of the problems (23),* $j = 1, \ldots, 8$, *yield zero.*

Proof. First, consider a box which is outside of the WCW. According to Lemma 1 for all positions p inside this box, problem (14) is unbounded. Since this is a maximization problem, the solution of its relaxed form in Eq. (21) provides an upper bound to its solution, which means that problem (21) is also unbounded whenever the box is outside the WCW. On the other hand, the solution to problem (14) is the maximum outcome of the eight linear programs of problem (compact primal). Hence, at least one of the eight distinct linear programs in Eq. (23) is unbounded whenever the box is outside of the WCW. Second, $\begin{bmatrix} \mu_0 & \rho_0 & \tau_0 & \mu^T & \eta^T & \rho^T & \tau^T & \chi^T & \psi^T & \delta \end{bmatrix}^T = \mathbf{0}_{16}$ is always feasible for problem (21), which implies that whenever all positions $\mathbf{p}$ of the given box are inside the WCW, problem (21) yields zero. Since the solution to problem (21) is the maximum outcome of the eight distinct LPs of Eq. (23) and $\xi_j = 0_{16}$, $j = 1, \ldots, 8$ is always feasible, then a given box is fully inside the WCW whenever all these LPs yield zero.

Hence, problem (23) provides a sufficient condition for a box to lie completely inside the WCW. This condition may be used to compute a *contracted* WCW, namely, a subset of the Cartesian workspace that is guaranteed to lie inside the WCW. To illustrate this, consider Fig. 3, which shows a sample PPCDM drawn from an article by Stump and Kumar [12]. The parameters of the considered PPCDM are given in Table 1.

Table 1 Geometric parameters of the assumed PPCDM

i	1	2	3	4
$\mathbf{a}_i^T$	[0 0]	[6 0]	[6 5]	[0 5]
$\mathbf{b}_i^T$	[−0.5 0]	[0.5 0]	[0.5 0.5]	[−0.5 0.5]

We then divide the Cartesian space into boxes that cover the interval -0.03 rad $\leq \phi \leq 0.03$ rad along the ϕ axis and that have edge of length 0.1 m along the x and y axes. We solve problem (compact primal) for each of these boxes and keep only those for which the maximum is 0. We obtain the contracted WCW, which is shown in Fig. 4, along with cross sections of the exact WCW. Evidently, this contracted WCW is the intersection of the constant orientation WCWs (COWCWs) corresponding to all orientations within the given range. Smaller boxes would have lead to a closer estimate of the WCW, as the convex relaxation (20) then forms a tighter approximation of (18) and more close to real dexterous WCW.

As they were obtained in problem (23), the inequality constraints can always be satisfied by choosing $\xi_j = 0_{16}$. For the purpose of later assembling them, we would like these constraints to be feasible only if a given box is fully inside the WCW. To this end, we compute the Lagrange dual [25] of problem (23). In the case of linear programs, recall that either of the following cases may occur [26]:

(1) The primal problem admits a feasible solution and has an unbounded objective value, in which case the dual problem is infeasible.
(2) The dual problem admits a feasible solution and has an unbounded objective value, in which case the primal problem is infeasible.
(3) Both problems admit feasible solutions, in which case both problems have equal optimal values.
(4) Both problems are infeasible.

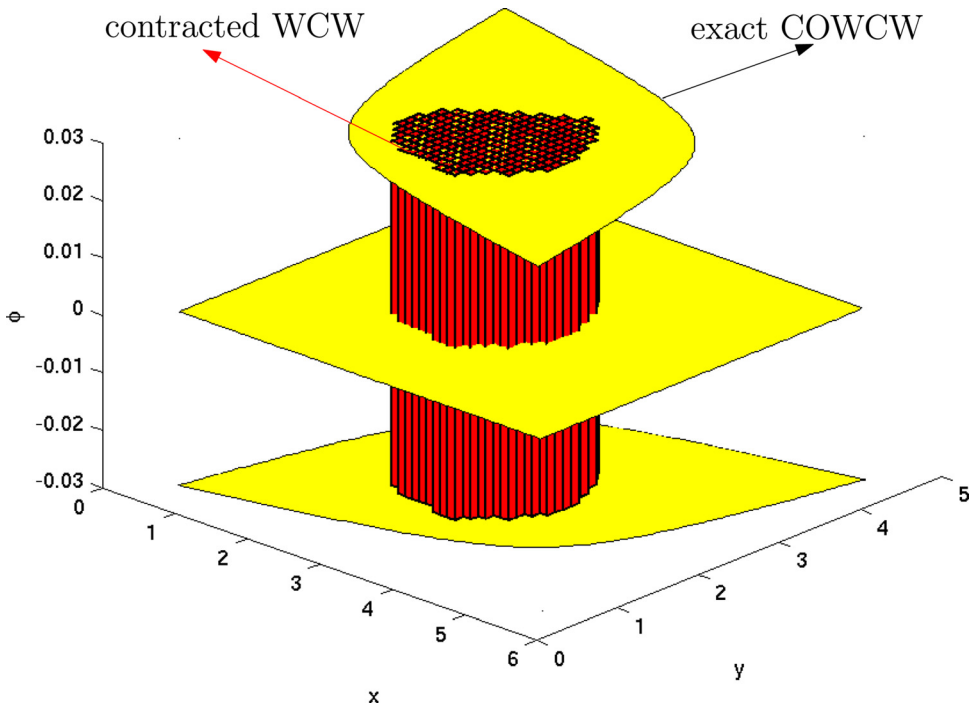

Fig. 4 Contracted WCW and cross sections of the exact WCW of the PPCDM geometry found in Ref. [12]

Let us start by writing the Lagrangian of problem (23)

$$L(\mathbf{x}_j, \xi_j) = \mathbf{x}_j^T(\mathbf{G}_j\xi_j) - \delta_j \tag{24}$$

where $\mathbf{x}_j \in_+ \mathbb{R}^{m+25}$ is the vector of Lagrange multipliers and $\mathbb{R}_+$ represents the non-negative real numbers. Hence, the Lagrange dual of our problem is that of maximizing $\theta(\mathbf{x}_j)$, where

$$\theta_j(\mathbf{x}_j) = \inf_{\xi_j}(\mathbf{x}_j, \xi_j), \quad j = 1, \ldots, 8 \tag{25}$$

Considering $\delta_j = \mathbf{e}_{16}^T\xi_j$, where $\mathbf{e}_{16} = [\mathbf{0}_{15}^T \quad 1]^T \in \mathbb{R}^{16}$, and substituting Eq. (24) into Eq. (25) gives

$$\theta_j(\mathbf{x}_j) = \inf_{\xi_j}(\mathbf{x}_j^T\mathbf{G}_j - \mathbf{e}_{16}^T)\xi_j \tag{26}$$

Clearly,

$$\theta_j(\mathbf{x}_j) = \begin{cases} 0 & \text{if } \mathbf{G}_j^T\mathbf{x}_j = \mathbf{e}_{16} \\ -\infty & \text{otherwise} \end{cases} \tag{27}$$

Hence, the dual problem of problem (23) can be stated as the following feasibility problem:

$$\begin{aligned} &\text{satisfy} \quad \mathbf{G}_j^T\mathbf{x}_j - \mathbf{e}_{16} = \mathbf{0}_{16}, \\ &\qquad\qquad \mathbf{x}_j \succeq \mathbf{0}_{m+25}, \quad j = 1, \ldots, 8 \\ &\text{over} \qquad\quad \mathbf{x}_j \end{aligned} \tag{28}$$

The last equality constraint of this linear program implies $x_{j,1} = 1$, $j = 1, \ldots, 8$, where $x_{j,1}$ represents the first element of the Lagrange multiplier $\mathbf{x}_j$. Substituting this in Eq. (28) eliminates $\mathbf{x}_{j,1}$ as a variable and reduces the number of the equality constraints from 16 to 15 which yields

$$\begin{aligned} &\text{satisfy} \quad \mathbf{R}_j\mathbf{y}_j + \mathbf{g} = \mathbf{0}_{15}, \\ &\qquad\qquad \mathbf{y}_j \succeq \mathbf{0}_{m+24}, \quad j = 1, \ldots, 8 \\ &\text{over} \qquad\quad \mathbf{y}_j \end{aligned} \tag{29}$$

where $\mathbf{y}_j \in \mathbb{R}_+^{m+24}$ represents the vector of Lagrange multipliers after eliminating the last equality constraint of Eq. (28).

Problem (29) is equivalent to its primal problems (23) but it is feasible when all problems (23) are zero and infeasible when any of those is unbounded. These correspond to cases 3. and 1., respectively, of the primal–dual relationships enumerated above. We may combine all of these problems just into one in order to verify whether a given box $\mathcal{B}$ is inside the WCW of a given PPCDM for a given range of orientation angles. This can be done by summing the objective values of these problems while considering all of their constraints together as follows:

$$\begin{aligned} &\text{satisfy} \quad \mathbf{R}_j\mathbf{y}_j + \mathbf{g} = \mathbf{0}_{15}, \quad j = 1, \ldots, 8 \\ &\qquad\qquad \mathbf{y}_j \succeq \mathbf{0}_{m+24}, \quad j = 1, \ldots, 8 \\ &\text{over} \qquad\quad \mathbf{y}_j, \quad j = 1, \ldots, 8 \end{aligned} \tag{30}$$

Notice that Eq. (29) represents eight distinct linear programs while Eq. (30) represents only one. Equation (30) may now be regarded as a single feasibility problem of 120 equality constraints and $8m + 192$ non-negative variables. If there is a feasible solution to this problem, then the given box $\mathcal{B}$ is inside the WCW. Having this information, we can now turn our attention to the synthesis problem.

5 A Formulation for the Problem of Synthesizing a PPCDM

Problem (30) serves as a building brick to solve the dimensional synthesis of PPCDMs. Suppose, we are interested in finding a PPCDM geometry whose WCW contains a given box $\mathcal{B}$ within a

given range of orientation angles. In order to solve this problem, we introduce the nonlinear feasibility problem

$$\begin{aligned} &\text{satisfy} && \mathbf{R}_j\mathbf{y}_j + \mathbf{g} = \mathbf{0}_{15}, \quad j = 1,\ldots,8 \\ &&& \mathbf{y}_j \succeq \mathbf{0}_{m+24}, \quad j = 1,\ldots,8 \\ &&& \underline{\mathbf{a}} \preceq \mathbf{a}_i \preceq \overline{\mathbf{a}}, \quad \underline{\mathbf{b}} \preceq \mathbf{b}_i \preceq \overline{\mathbf{b}}, \quad i = 1,\ldots,m \\ &\text{over} && \mathbf{y}_j \in \mathbb{R}^{m+24}, \mathbf{a}_i \in \mathbb{R}^2, \mathbf{b}_i \in \mathbb{R}^2 \end{aligned} \tag{31}$$

Here, $\underline{\mathbf{a}}$, $\overline{\mathbf{a}}$, $\underline{\mathbf{b}}$, and $\overline{\mathbf{b}}$ are lower and upper bounds on the positions of the base and MP attachments points, which would otherwise be drawn to infinity during the solution process. If it exists, the associated solution of problem (31) yields a PPCDM geometry whose WCW is guaranteed to include the prescribed box $\mathcal{B}$. On the other hand, the absence of a solution to this problem does not imply that there is no possible PPCDM geometry containing $\mathcal{B}$. Hence, this method lacks practicality, since failing to obtain a feasible solution does not provide any information regarding a *good* but *not perfect* geometry. For this reason, we add an objective function over the constraints, which is thought to be more attractive to the designers. This is the main concern of Sec. 5.1.

5.1 Introducing an Objective Function. Suppose, we want to find the geometry of a PPCDM whose WCW includes a given box. Evidently, if we use a scaled version of this box in problem (31) and can find a geometry of a PPCDM whose WCW allows for a scaling factor above 1, then the original problem is solved. Quite naturally, the idea is to consider the scaling factor as an objective function to be maximized. If, at the optimum point this factor is smaller than 1, then the designer is left with the best infeasible solution.

This scaling process is depicted in Fig. 5 for a prescribed box. The box $\mathcal{B}\prime$ with dashed lines in blue is the scaled image of the smaller one with solid lines in red. The scaling factor is s and the scaling point is C.

From this figure, we can obtain the lower-left and upper-right coordinates of the scaled box $\mathcal{B}'$ as

$$\underline{\mathbf{p}}\prime = \mathbf{p}_c + s(\underline{\mathbf{p}} - \mathbf{p}_c) \quad \text{and} \quad \overline{\mathbf{p}}' = \mathbf{p}_c + s(\overline{\mathbf{p}} - \mathbf{p}_c) \tag{32}$$

respectively. Vector $\mathbf{p}_c$ and scalar s represent the position of the scaling point C and the scaling factor, respectively. If we consider the centroid of the box as the scaling point, then $\mathbf{p}_c = \frac{1}{2}(\overline{\mathbf{p}} + \underline{\mathbf{p}})$. Introducing this objective function enables us to develop a nonlinear program for the dimensional synthesis of PPCDMs.

5.2 A Nonlinear Program for the Dimensional Synthesis of PPCDMs. We now turn the feasibility problem (31) into a nonlinear program where $\mathbf{R}'_j$ is obtained by substituting $\overline{\mathbf{p}}'$ and $\underline{\mathbf{p}}'$ for $\overline{\mathbf{p}}$ and $\underline{\mathbf{p}}$, respectively, in the expression of $\mathbf{R}_j$ given in problem (23). Moreover, to ensure that $\underline{\mathbf{p}}'$ and $\overline{\mathbf{p}}'$ remain the lower-left and upper-right corners of the scaled box, we constrain the scaling factor s to non-negative real numbers. Hence, the corresponding nonlinear program to solve the synthesis of PPCDMs for a prescribed box is

$$\begin{aligned} &\text{maximize} && s \\ &\text{subject to} && \mathbf{R}'_j\mathbf{y}_j + \mathbf{g} = \mathbf{0}_{15} \\ &&& \underline{\mathbf{p}}' - \mathbf{p}_c - s(\underline{\mathbf{p}} - \mathbf{p}_c) = \mathbf{0}_2 \\ &&& \overline{\mathbf{p}}' - \mathbf{p}_c - s(\overline{\mathbf{p}} - \mathbf{p}_c) = \mathbf{0}_2 \\ &&& \underline{\mathbf{a}} \preceq \mathbf{a}_i \preceq \overline{\mathbf{a}}, \quad \underline{\mathbf{b}} \preceq \mathbf{b}_i \preceq \overline{\mathbf{b}}, \quad i = 1,\ldots,m \\ &&& \mathbf{y}_j \succeq \mathbf{0}_{m+24}, \quad j = 1,\ldots,8 \\ &&& s \geq 0 \\ &\text{over} && \mathbf{y}_j \in \mathbb{R}^{m+24}, \ \mathbf{a}_i \in \mathbb{R}^2, \ \mathbf{b}_i \in \mathbb{R}^2, \ s \in \mathbb{R} \end{aligned} \tag{33}$$

Since the main challenge of the synthesis problem consists in finding a PPCDM whose WCW contains a prescribed workspace with an irregular shape, we may estimate such a shape with multiple boxes. To this end, we use interval analysis [23] as a tool to overestimate the prescribed workspace with a set of boxes. The procedure consists in considering a large rectangle that includes the prescribed workspace. Dividing this large rectangle along its longer edge provides two new boxes, which are examined to verify whether they are inside or outside the prescribed workspace. For each box, if we find it completely inside or outside of the prescribed workspace, then we mark it as a certain box and put it aside. Otherwise, the box is an uncertain box and must be divided into smaller boxes. Again, we examine these new boxes to verify whether they are completely inside or outside the prescribed

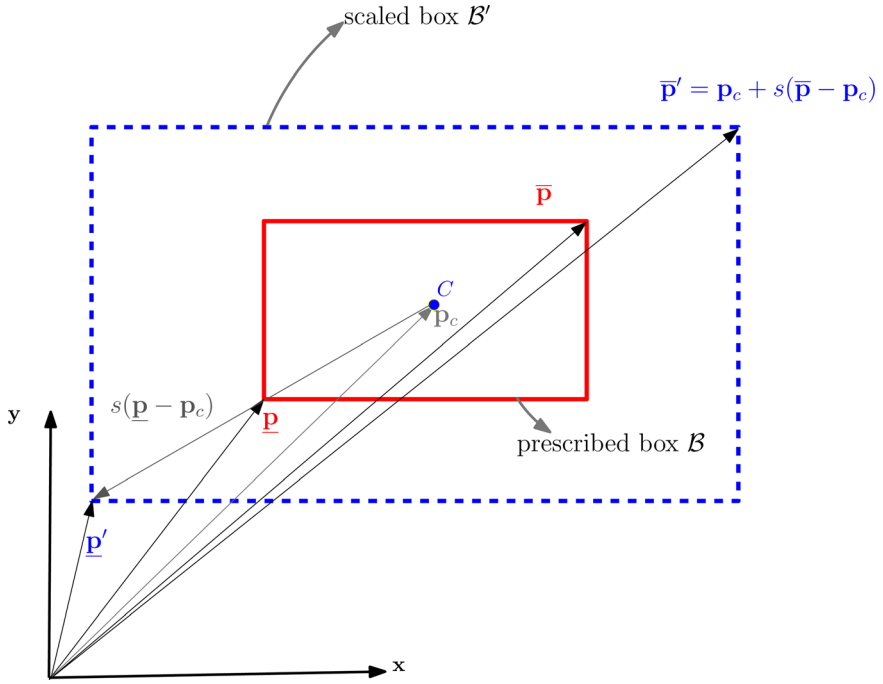

Fig. 5 An scaled-up box and its corresponding parameters

workspace. The procedure ends whenever the total number of certain and uncertain boxes reaches a given maximum number of boxes. Evidently, a larger number of boxes provides a more accurate estimate of the prescribed workspace. Also, notice that it may prove useful to divide even a rectangular prescribed WCW, into smaller boxes, since the proposed convex relaxations are tighter over smaller boxes, and may thus lead to a larger maximum s^* of the scaling factor, as we mentioned in Sec. 4.

In order to solve the dimensional synthesis problem for a prescribed workspace composed of multiple boxes, the formulation (33) can be developed to include several boxes. This is done by considering the constraints corresponding to each box while attempting to maximize a common scaling factor s with respect to a common scaling point, which may be the centroid of the approximated WCW. Symbolically, we obtain

$$\begin{aligned}
&\text{maximize} && s\\
&\text{subject to} && \mathbf{R}_{k,j}\mathbf{y}_{k,j}+\mathbf{g}=\mathbf{0}_{15}\\
&&& \underline{\mathbf{p}}'_k-\mathbf{p}_c-s(\underline{\mathbf{p}}_k-\mathbf{p}_c)=\mathbf{0}_2\\
&&& \overline{\mathbf{p}}'_k-\mathbf{p}_c-s(\overline{\mathbf{p}}_k-\mathbf{p}_c)=\mathbf{0}_2\\
&&& \underline{\mathbf{a}}\preceq\mathbf{a}_i\preceq\overline{\mathbf{a}},\ \ \underline{\mathbf{b}}\preceq\mathbf{b}_i\preceq\overline{\mathbf{b}},\ \ i=1,\ldots,m\\
&&& s\geq 0\\
&&& \mathbf{y}_{k,j}\succeq\mathbf{0}_{m+24},\ \ j=1,\ldots,8,\ \ k=1,\ldots,n\\
&\text{over} && \mathbf{y}_{k,j}\in\mathbb{R}^{m+24},\ \ \mathbf{a}_i\in\mathbb{R}^2,\ \ \mathbf{b}_i\in\mathbb{R}^2,\ s\in\mathbb{R}
\end{aligned}\tag{34}$$

where n is the number of boxes. Notice that we must consider the lower-left corner $\underline{\mathbf{p}}'_k$ and upper-right corner $\overline{\mathbf{p}}'_k$ of each scaled box to construct the matrix $\mathbf{R}_{k,j}$. This forms a nonlinear program with $8n(m+24)+4m+1$ variables, $120n$ equality constraints, and $8n(m+24)+8m+1$ inequality constraints. Evidently, depending on the number of boxes required, this problem can become a large-scale nonlinear program. Nevertheless, problem (34) provides us with a tool to find a PPCDM whose WCW includes a prescribed workspace within a given range of orientations. As the problem (34) is nonconvex, the geometry it yields depends on the chosen initial guess. We illustrate this with a synthesis example as follows.

Example 1. Dimensional synthesis of PPCDMs for a given box and a given range of orientations.

Suppose, we are given a prescribed rectangular WCW with lower-left and upper-right coordinates $\underline{\mathbf{p}}=[0.4\quad 0.4]^T$ and $\overline{\mathbf{p}}=[0.55\quad 0.55]^T$, respectively and the range of rotation angles is $-\pi/3\leq\phi\leq\pi/3$. We want to find a PPCDM whose WCW within this given range of rotation angles includes this prescribed workspace. The assumed upper and lower bounds for the geometry of the mechanism are given in Table 2.

The number of cables is set to $m=4$, which is the minimum necessary for a WCW to exist. In order to tighten the constraints on the variables defined in Sec. 4 and obtain a PPCDM with a larger WCW, we divide this prescribed box into $n=9$ similar boxes with edges of 0.05 in the xy plane.

One of the most popular methods of finding local maxima to problem (34) is to use the standard MATLAB solvers, which are called through the *fmincon* function. Unfortunately, we found this solver too slow when applied to the obtained formulation for the synthesis of PPCDMs. Also, as the function cannot accept sparse matrices, it often encounters memory errors, depending on the available memory of the computer used and on the number of boxes n. In order to circumvent these problems, we decided instead to use our own specific MATLAB implementation of the *penalty successive linear programming* (PSLP) *algorithm* [26] to solve the problem. The algorithm is in the class of SLP algorithms, which employ the l_1-norm, i.e., the absolute value in the direction-finding subproblem, which becomes a linear program based on first-order Taylor series approximations to the objective and constraint functions. These linear-programming subproblems were solved using MATLAB's *linprog* command where the sparsity pattern could be exploited to improve the speed and avoid memory errors. From this linear program, PSLP algorithm converges toward a local maximum of the principal problem, by means of a hypercube shaped trust region approach.

Table 2 Upper and lower bounds on the geometry of the PPCDM

$\underline{\mathbf{a}}^T$	$\overline{\mathbf{a}}^T$	$\underline{\mathbf{b}}^T$	$\overline{\mathbf{b}}^T$
[0 0]	[1 1]	[−0.2 −0.2]	[0.2 0.2]

In order to solve the current example, we used the parameters of the PSLP algorithm that are proposed in Ref. [26]. The algorithm was implemented in MATLAB 7.6.0 *R2008a* on a PC with Intel(R) Core(TM)2 CPU 6400 @ 2.13 GHz, and 4 Gbyte RAM. In order to find a better local optimum, the problem is solved repeatedly for 100 initial guesses, which were generated using uniformly distributed pseudo random numbers, produced by the *rand* function in MATLAB. In order to ensure that the produced initial guesses cover well the feasible set, we use the following formulation to produce the initial geometry:

$$\begin{aligned}
\mathbf{a}_i&=\underline{\mathbf{a}}+\text{diag}(\overline{\mathbf{a}}-\underline{\mathbf{a}})\alpha_i\\
\mathbf{b}_i&=\underline{\mathbf{b}}+\text{diag}(\overline{\mathbf{b}}-\underline{\mathbf{b}})\beta_i,\quad i=1,\ldots,m
\end{aligned}\tag{35}$$

where $\alpha_i\in\mathbb{R}^2$ and $\beta_i\in\mathbb{R}^2$ are random numbers produced by *rand* function of MATLAB. Figure 6 shows the histogram of the obtained results for the generated points.

As can be seen from this figure, 32% of the generated initial guesses end with the scaling factor greater than 1, which means that the WCWs of the corresponding PPCDMs are guaranteed to include the prescribed box for the given range of orientation angles. As for the remaining 68% initial guesses we cannot draw conclusions, but the prescribed box may yet be inside of the resulting WCW, as the proposed method always underestimates the WCW.

One of the robot geometries obtained by applying the PSLP algorithm to problem (34) is shown in Fig. 7. This PPCDM corresponds to the best scaling factor obtained, namely $s^*=2.8273$.

The corresponding scaled boxes and WCW cross sections are depicted in Fig. 8. As can be seen, the scaled boxes and, consequently, the prescribed boxes are entirely inside the WCW of the mechanism obtained. The exact initial guess and final optimum are reported in Tables 3 and 4, respectively. For this example, it took 42 min to obtain the final solution by using the desktop computer mentioned at the beginning of this example. Figure 9 shows the evolution of the scaling factor during the solution procedure. Notice that the initial decrease in s is a result of the PSLP algorithm first seeking to satisfy the constraints at the expense of objective.

Example 2. Synthesizing a PPCDM for a nonrectangular prescribed workspace.

Suppose, we want to find the geometry of a PPCDM whose WCW for the given range of orientations, $-\pi/6\leq\phi\leq\pi/6$, includes the elliptic desired workspace $\mathcal{E}_d$ represented by $(x-3.5)^2/1.6^2+(y-3)^2/1.1^2\leq 1$. We approximate this prescribed WCW by means of interval analysis, as explained in the second paragraph of Sec. 5.2. The resulting approximation is depicted in Fig. 10.

In order to ensure that the multiple boxes will cover entirely the prescribed WCW, we overestimate the desired WCW with $\mathcal{E}_e$ represented by $(x-3.5)^2/1.9^2+(y-3)^2/1.33^2\leq 1$ whose corresponding certain boxes inside cover $\mathcal{E}_d$. For this estimation, we have $n=32$ prescribed boxes and the selected lower and upper bounds for the base and moving platform anchor points are shown in Table 5.

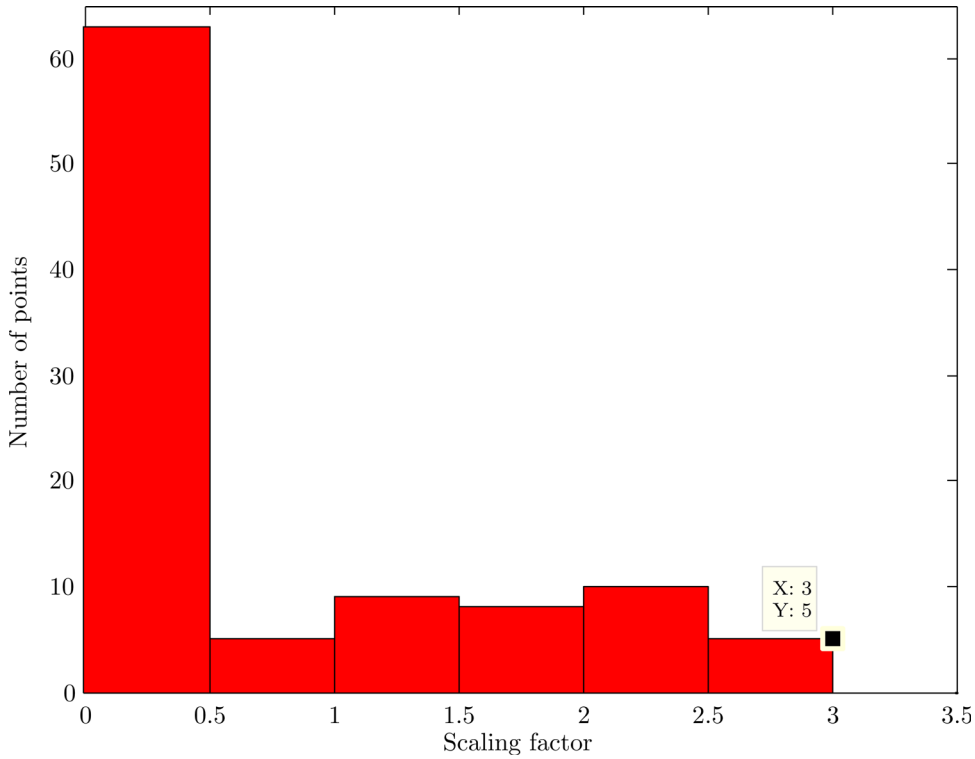

Fig. 6 Distribution of the randomly generated initial points with the obtained scaling factors

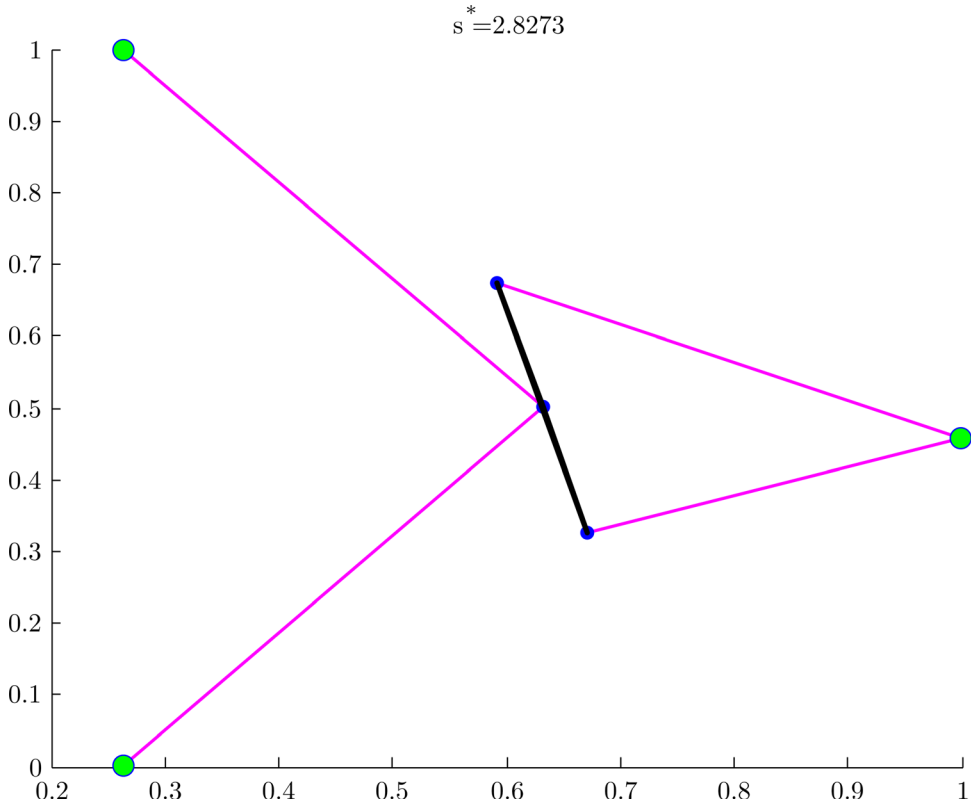

Fig. 7 One of the obtained PPCDMs

The number of cables is set to $m = 5$ and we solve this problem using the PSLP algorithm for 50 initial uniformly distributed random points.

The best solution obtained using these initial guesses is $s^* = 1.3832$ and its corresponding geometry and COWCW for the angles $\phi = -\pi/6, 0, \pi/6$ are depicted in Fig. 11. Table 6 shows the coordinates of the attachment and anchor points corresponding to the initial guesses and its resulting solution.

As can be seen from this figure, the scaled boxes and consequently the prescribed ellipse $\mathcal{E}_d$ are all included inside the WCW of the obtained PPCDM for the provided range of orientations.

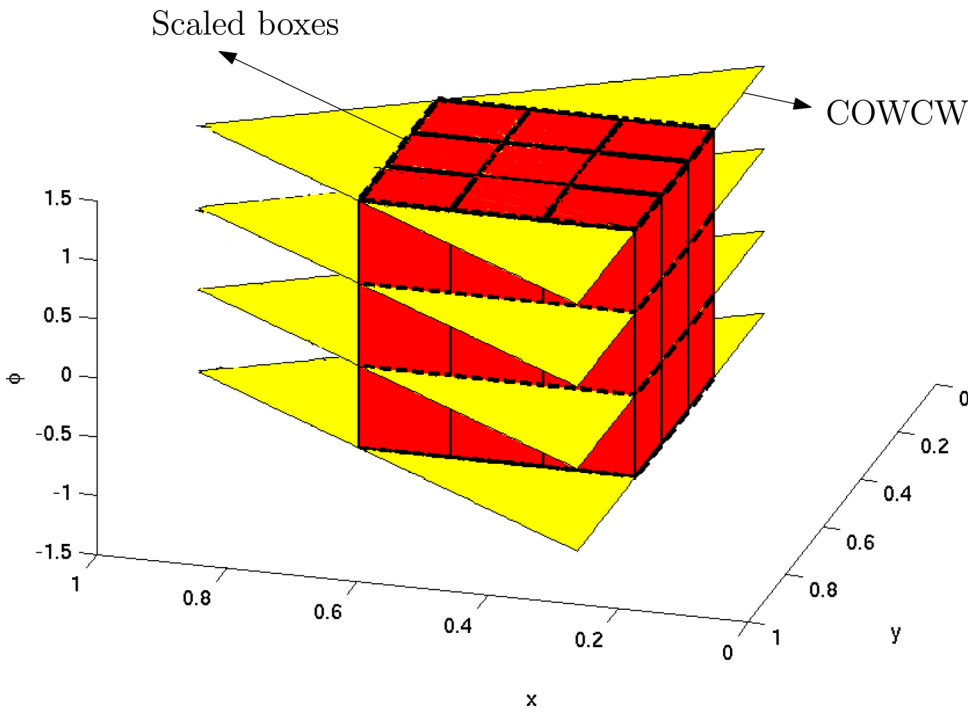

Fig. 8 Scaled boxes and COWCWs for the orientations $\phi = -\pi/3, -\pi/9, \pi/9, \pi/3$

Table 3 Initial geometry

i	$\mathbf{a}_{i,0}^T$	$\mathbf{b}_{i,0}^T$
1	[0.4972 0.1391]	[0.1813 − 0.1943]
2	[0.5965 0.5021]	[−0.0612 − 0.1840]
3	[0.1940 0.2865]	[−0.1971 0.1408]
4	[0.3583 0.2099]	[0.1447 0.0457]

Table 4 Final geometry

i	$\mathbf{a}_{i,f}^T$	$\mathbf{b}_{i,f}^T$
1	[0.2627 0.0000]	[0.0000 0.0000]
2	[1.0000 0.4566]	[0.0399 − 0.1748]
3	[1.0000 0.4566]	[−0.0399 0.1748]
4	[0.2627 1.0000]	[0.0000 0.0000]

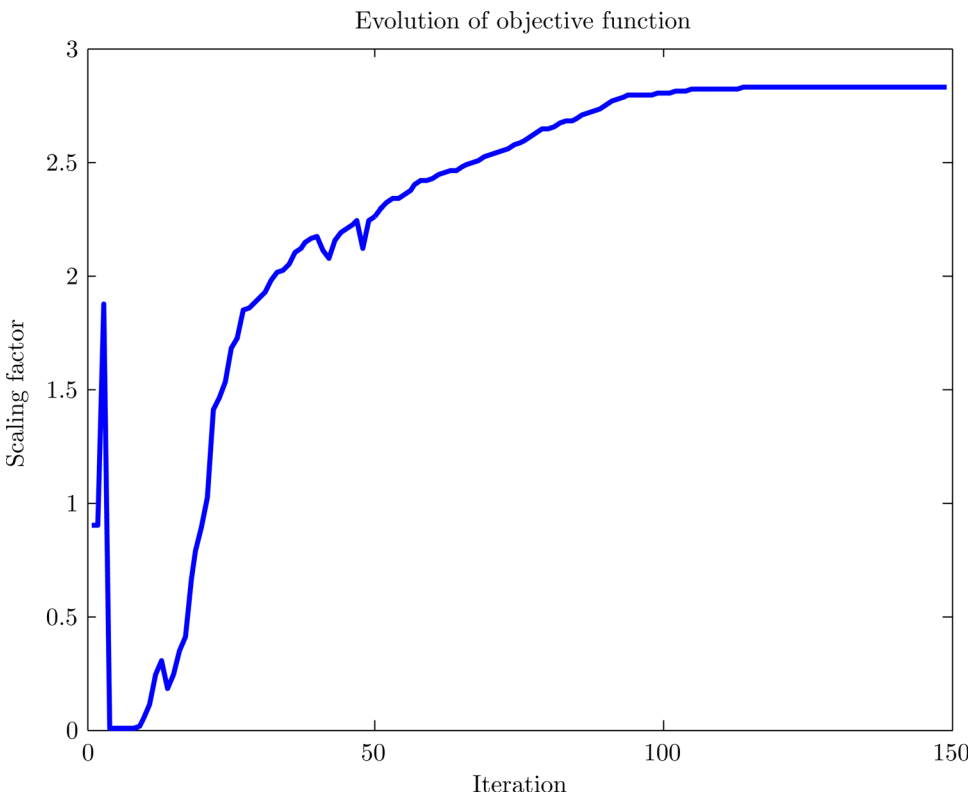

Fig. 9 Evolution of scaling factor

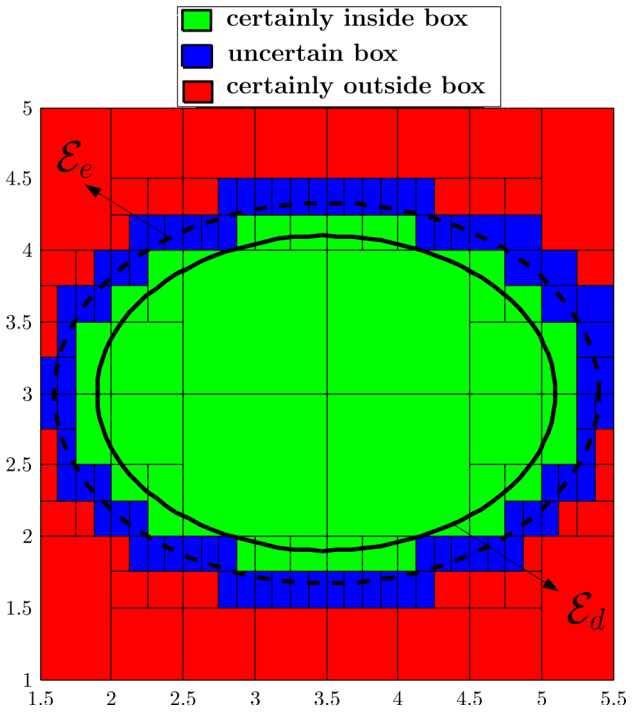

Fig. 10 Approximated desired workspace with multiple boxes

6 Discussion

Splitting the given interval of orientation angles into several subintervals and providing tighter relaxations on trigonometric and trilinear terms [27,28] may provide better approximations of the WCW. Applying the procedures presented in this paper to the wrench feasible concept may lead us to the designs of PPCDMs whose wrench-feasible workspaces include a prescribed workspace. This is more interesting from a practical point of view, as tensions in cables are limited to maximum possible tensions due to their limited strength. Finding the global optimum for the developed optimization problems will lead to the best possible designs of PPCDMs. Applying the branch and bound method [25] may lead to such global optima.

In this paper, we gave priority to the point-position rather than the orientation during the development of the formulation for the dimensional synthesis of PPCDMs. However, depending on the application, we may require a PPCDM that is capable of operating in wide ranges of orientations. Introducing a multi-objective function including scaling factors for both the point-position and the orientation seems to be a good method of turning the obtained feasibility problem into a nonlinear program.

Moreover, the extension of the proposed formulation to spatial parallel cable-driven mechanisms may provide a good tool for the synthesis of such devices. Even better, our intuition is that the same approach could be applied to the dimensional synthesis of conventional mechanisms. All these ideas will be the topics of further reports.

Table 5 Upper and lower bounds on the geometry of the PPCDM for the prescribed WCW

$\underline{\mathbf{a}}^T$	$\overline{\mathbf{a}}^T$	$\underline{\mathbf{b}}^T$	$\overline{\mathbf{b}}^T$
[0 0]	[6 5]	$[-0.5 \; -0.5]$	[0.5 0.5]

7 Conclusions

A method for the dimensional synthesis of PPCDMs was proposed. To achieve this goal, an optimization problem was first introduced to verify whether a given pose is inside the WCW of a

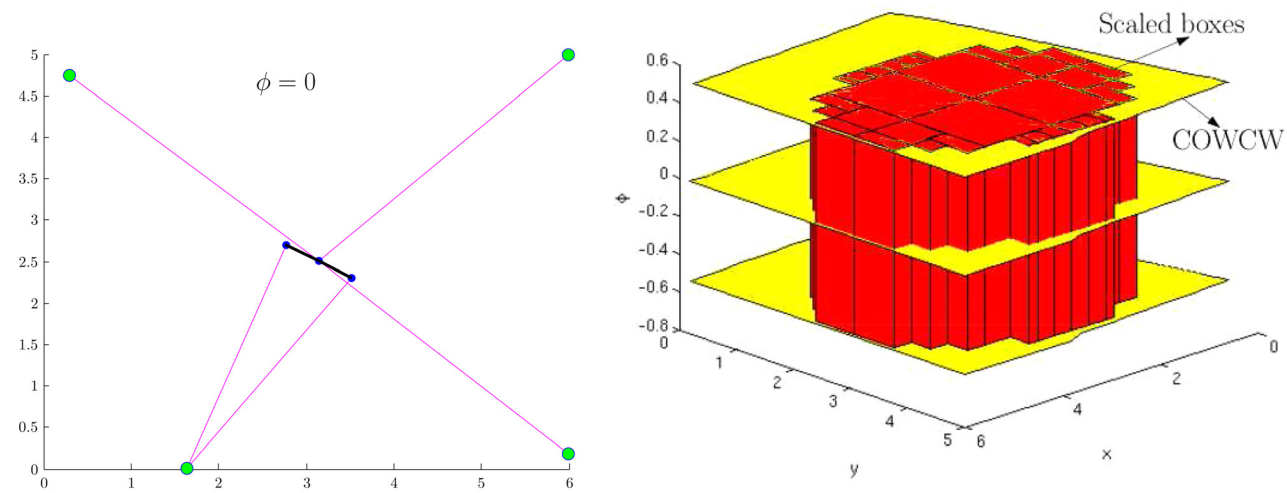

(a) The obtained PPCDM (b) COWCWs for the orientation angles $\phi = -\pi/6, 0, \pi/6$

Fig. 11 The obtained PPCDM and its corresponding COWCW

Table 6 Initial and final geometries

i	$\mathbf{a}_{i,0}^T$	$\mathbf{b}_{i,0}^T$	i	$\mathbf{a}_{i,f}^T$	$\mathbf{b}_{i,f}^T$
1	[0.4884 0.3551]	[0.1656 0.2700]	1	[1.6382 0.0033]	[0.3774 – 0.1935]
2	[2.9599 2.2603]	[0.6799 0.5078]	2	[5.9999 4.9995]	[0.0000 0.0000]
3	[1.7818 1.3436]	[0.0239 0.8245]	3	[5.9999 0.1784]	[0.0000 0.0000]
4	[0.7605 0.4252]	[0.3723 0.3152]	4	[1.6382 0.0033]	[−0.3774 0.1935]
5	[0.9550 3.8578]	[0.7498 0.1322]	5	[0.2906 4.7378]	[0.0000 0.0000]

given PPCDM. We then relaxed this problem over a box in the workspace, which leads us to a sufficient condition for this box to be inside the WCW of a given PPCDM for a given range of orientations. These mathematical conditions allowed the formulation of a nonlinear program in which the scale of the prescribed workspace is maximized while being constrained inside the PPCDM WCW. The robot geometry being included in the decision variables of the nonlinear program, this optimization problem is a useful tool sought for the dimensional synthesis of PPCDMs. The value of the scaling factor at the optimum indicates whether the prescribed box is inside the WCW for the given range of orientation angles. Solving the problem for different initial guesses may provide us a larger scaling factor, and thus a larger WCW.

Appendix: Expressions of Matrix $\mathbf{R}_j$ and Vector $\mathbf{g}$

The vector $\mathbf{g} \in \mathbb{R}^{15}$ and the matrix $\mathbf{R}_j \in \mathbb{R}^{15\times(m+24)}$ appearing in Eq. (23) are

$$\mathbf{g} \equiv \begin{bmatrix} 0 & -\mathbf{1}_m^T\mathbf{u} & -\mathbf{1}_m^T\mathbf{v} & -\mathbf{1}_m^T\mathbf{A}^T & m\mathbf{1}_2^T & \mathbf{1}_m^T\mathbf{B}^T & \mathbf{1}_m^T\mathbf{B}^T\mathbf{E}^T & \mathbf{1}_m^T\mathbf{B}^T\mathbf{E}^T & -\mathbf{1}_m^T\mathbf{B}^T \end{bmatrix}^T \in \mathbb{R}^{15}$$

$$\mathbf{R}_j \equiv \begin{bmatrix} \mathbf{0}_{m\times1} & -\mathbf{u} & -\mathbf{v} & -\mathbf{A}^T & \mathbf{1}_m\mathbf{1}_2^T & \mathbf{B}^T & \mathbf{B}^T\mathbf{E}^T & \mathbf{B}^T\mathbf{E}^T & -\mathbf{B}^T \\ \mathbf{0}_{2\times1} & \mathbf{0}_{2\times1} & \mathbf{0}_{2\times1} & \mathrm{diag}(\sigma_j)\mathrm{diag}(\underline{\mathbf{p}}) & -\mathrm{diag}(\sigma_j) & \mathbf{0}_{2\times2} & \mathbf{0}_{2\times2} & \mathbf{0}_{2\times2} & \mathbf{0}_{2\times2} \\ \mathbf{0}_{2\times1} & \mathbf{0}_{2\times1} & \mathbf{0}_{2\times1} & -\mathrm{diag}(\sigma_j)\mathrm{diag}(\overline{\mathbf{p}}) & \mathrm{diag}(\sigma_j) & \mathbf{0}_{2\times2} & \mathbf{0}_{2\times2} & \mathbf{0}_{2\times2} & \mathbf{0}_{2\times2} \\ \mathbf{0}_{2\times1} & \mathbf{0}_{2\times1} & \mathbf{0}_{2\times1} & \underline{c}\mathrm{diag}(\sigma_j) & \mathbf{0}_{2\times2} & -\mathrm{diag}(\sigma_j) & \mathbf{0}_{2\times2} & \mathbf{0}_{2\times2} & \mathbf{0}_{2\times2} \\ \mathbf{0}_{2\times1} & \mathbf{0}_{2\times1} & \mathbf{0}_{2\times1} & -\bar{c}\mathrm{diag}(\sigma_j) & \mathbf{0}_{2\times2} & \mathrm{diag}(\sigma_j) & \mathbf{0}_{2\times2} & \mathbf{0}_{2\times2} & \mathbf{0}_{2\times2} \\ \mathbf{0}_{2\times1} & \mathbf{0}_{2\times1} & \mathbf{0}_{2\times1} & \underline{s}\mathrm{diag}(\sigma_j) & \mathbf{0}_{2\times2} & \mathbf{0}_{2\times2} & -\mathrm{diag}(\sigma_j) & \mathbf{0}_{2\times2} & \mathbf{0}_{2\times2} \\ \mathbf{0}_{2\times1} & \mathbf{0}_{2\times1} & \mathbf{0}_{2\times1} & -\bar{s}\mathrm{diag}(\sigma_j) & \mathbf{0}_{2\times2} & \mathbf{0}_{2\times2} & \mathrm{diag}(\sigma_j) & \mathbf{0}_{2\times2} & \mathbf{0}_{2\times2} \\ \sigma_{0,j}\underline{\alpha} & \mathbf{0}_{2\times1} & \mathbf{0}_{2\times1} & \mathbf{0}_{2\times2} & \mathbf{0}_{2\times2} & \mathbf{0}_{2\times2} & \mathbf{0}_{2\times2} & -\sigma_{0,j}\mathbf{1}_{2\times2} & \mathbf{0}_{2\times2} \\ -\sigma_{0,j}\overline{\alpha} & \mathbf{0}_{2\times1} & \mathbf{0}_{2\times1} & \mathbf{0}_{2\times2} & \mathbf{0}_{2\times2} & \mathbf{0}_{2\times2} & \mathbf{0}_{2\times2} & \sigma_{0,j}\mathbf{1}_{2\times2} & \mathbf{0}_{2\times2} \\ \sigma_{0,j}\underline{\beta} & \mathbf{0}_{2\times1} & \mathbf{0}_{2\times1} & \mathbf{0}_{2\times2} & \mathbf{0}_{2\times2} & \mathbf{0}_{2\times2} & \mathbf{0}_{2\times2} & \mathbf{0}_{2\times2} & -\sigma_{0,j}\mathbf{1}_{2\times2} \\ -\sigma_{0,j}\overline{\beta} & \mathbf{0}_{2\times1} & \mathbf{0}_{2\times1} & \mathbf{0}_{2\times2} & \mathbf{0}_{2\times2} & \mathbf{0}_{2\times2} & \mathbf{0}_{2\times2} & \mathbf{0}_{2\times2} & \sigma_{0,j}\mathbf{1}_{2\times2} \\ \sigma_{0,j} & -\sigma_{0,j} & 0 & \mathbf{0}_{1\times2} & \mathbf{0}_{1\times2} & \mathbf{0}_{1\times2} & \mathbf{0}_{1\times2} & \mathbf{0}_{1\times2} & \mathbf{0}_{1\times2} \\ -\sigma_{0,j}\bar{c} & \sigma_{0,j} & 0 & \mathbf{0}_{1\times2} & \mathbf{0}_{1\times2} & \mathbf{0}_{1\times2} & \mathbf{0}_{1\times2} & \mathbf{0}_{1\times2} & \mathbf{0}_{1\times2} \\ \sigma_{0,j} & 0 & -\sigma_{0,j} & \mathbf{0}_{1\times2} & \mathbf{0}_{1\times2} & \mathbf{0}_{1\times2} & \mathbf{0}_{1\times2} & \mathbf{0}_{1\times2} & \mathbf{0}_{1\times2} \\ -\sigma_{0,j}\bar{s} & 0 & \sigma_{0,j} & \mathbf{0}_{1\times2} & \mathbf{0}_{1\times2} & \mathbf{0}_{1\times2} & \mathbf{0}_{1\times2} & \mathbf{0}_{1\times2} & \mathbf{0}_{1\times2} \end{bmatrix}^T \in \mathbb{R}^{15\times m+24}$$

References

[1] Riechel, A. T., Bosscher, P., Lipkin, H., and Ebert-Uphoff, I., 2004, "Concept Paper: Cable-Driven Robots for Use in Hazardous Environments," 10th International Topical Meeting on Robotics and Remote Systems for Hazardous Environments, Gainesville, FL, USA.

[2] Bosscher, P., Williams, R. L., and Tummino, M., 2005, "A Concept for Rapidly Deployable Cable Robot Search and Rescue Systems," ASME IDETC/CIE, Long Beach, CA, USA.

[3] SkyCam, 2007, www.skycam.tv

[4] Borgstrom, P. H., Borgstrom, N. P., Stealey, M. J., Jordan, B., and Sukhatme, G. S., 2009, "Design and Implementation of NIMS3D, a 3-D Cabled Robot for Actuated Sensing Applications," IEEE Trans. Rob., **25**(2), pp. 325–339.

[5] Borgstrom, P. H., Jordan, B. J., Stealey, M. J., Sukhatme, G. S., Kaiser, W. J., and Batalin, M. A., 2009, "Nims-pl: A Cable-Driven Robot With Self-Calibration Capabilities," IEEE Trans. Rob., **25**(5), pp. 1005–1015.

[6] Gosselin, C., Poulin, R., and Laurendeau, D., 2008, "A Planar Parallel 3-dof Cable-Driven Haptic Interface," 12th World Multi-Conference on Systemics, Cybernetics and Informatics, Orlando, FL, USA, pp. 266–271.

[7] Williams, R. L., II, 1998, "Cable-Suspended Haptic Interface," Int. J. Virtual Reality, **3**(3), pp. 13–20.

[8] Kurtz, R., and Hayward, V., 1991, "Dexterity Measure for Tendon Actuated Parallel Mechanisms," IEEE International Conference on Advanced Robotics, Pisay, Italy, pp. 1141–1146.

[9] Ming, A., and Higuchi, T., 1994, "Study on Multiple Degree-of-Freedom Positioning Mechanism Using Wires (Part 1) Concept, Design and Control," Int. J. Jpn. Soc. Precis. Eng., **28**(2), pp. 131–138.

[10] Gosselin, C., Lefrançois, S., and Zoso, N., 2010, "Underactuated Cable-Driven Robots: Machine, Control and Suspended Bodies," *Brain, Body and Machine*, Vol. 83, J. Angeles, B. Boulet, J. J. Clark, J. Kövecses, and K. Siddiqi, eds., Springer, Berlin, pp. 311–323.

[11] Pham, C. B., Yeo, S. H., Yang, G., Kurbanhusen, M. S., and Chen, I.-M., 2006, "Force-Closure Workspace Analysis of Cable-Driven Parallel Mechanisms," Mech. Mach. Theory, **41**, pp. 53–69.

[12] Stump, E., and Kumar, V., 2006, "Workspaces of Cable-Actuated Parallel Manipulators," ASME J. Mech. Des., **128**(1), pp. 159–167.

[13] Fattah, A., and Agrawal, S., 2005, "On the Design of Cable-Suspended Planar Parallel Robots," ASME J. Mech. Des., **127**(5), pp. 1021–1028.

[14] Riechel, A. T., and Ebert-Uphoff, I., 2004, "Force-Feasible Workspace Analysis for Underconstrained, Point-Mass Cable Robots," IEEE International Conference on Robotics & Automation, New Orleans, LA, USA, pp. 4956–4962.

[15] McColl, D., and Notash, L., 2009, "Extension of Antipodal Theorem to Workspace Analysis of Planar Wire-Actuated Manipulators," Proceedings of the 5th IFToMM International Workshop, pp. 9–16.

[16] Gouttefarde, M., Daney, D., and Merlet, J. P., 2011, "Interval-Analysis-Based Determination of the Wrench-Feasible Workspace of Parallel Cable-Driven Robots," IEEE Trans. Rob., **27**(1), pp. 1–13.

[17] Hay, A. M., and Snyman, J. A., 2005, "Optimization of a Planar Tendon-Driven Parallel Manipulator for a Maximal Dextrous Workspace," Eng. Optimiz., **37**(3), pp. 217–236.

[18] Kolev, K., and Cremers, D., 2009, "Continuous Ratio Optimization via Convex Relaxation With Applications to Multiview 3D Reconstruction," IEEE

Computer Society Conference on Computer Vision and Pattern Recognition, Miami, FL, USA, pp. 1858–1864.
[19] Cafieri, S., Lee, J., and Liberti, L., 2010, "On Convex Relaxations of Quadrilinear Terms," J. Global Optim., **47**(4), pp. 661–685.
[20] Porta, J., Rose, L., and Thomas, F., 2009, "A Linear Relaxation Technique for the Position Analysis of Multiloop Linkages," IEEE Trans. Rob., **25**(2), pp. 225–239.
[21] Graham, T., Roberts, R., and Lippitt, T., 1998, "On the Inverse Kinematics, Statics, and Fault Tolerance of Cable-Suspended Robots," J. Rob. Syst., **15**(10), pp. 581–597.
[22] Dantzig, G., and Thapa, M., 2003, *Linear Programming: Theory and Extensions*, Springer, New York.
[23] Moore, R. E., Kearfott, R. B., and Cloud, M. J., 2009, *Introduction to Interval Analysis*, SIAM, Philadelphia, PA, USA.
[24] Sherali, H., and Tuncbilek, C. H., 1995, "A Reformulation-Convexification Approach for Solving Nonconvex Quadratic Programming Problems," J. Global Optim., **7**, pp. 1–31.
[25] Boyd, S., and Vandenberghe, L., 2004, *Convex Optimization*, Cambridge University Press, Cambridge, UK.
[26] Bazarra, M., Sherali, H., and Shetty, C., 2006, *Nonlinear Programming*, Wiley Interscience, Hoboken, NJ, USA.
[27] McCormick, G. P., 1976, "Computability of Global Solutions to Factorable Nonconvex Programs: Part I: Convex Underestimating Problems," Math. Program., **10**, pp. 147–175.
[28] Meyer, C. A., and Floudas, C. A., 2004, "Trilinear Monomials With Mixed Sign Domains: Facets of the Convex and Concave Envelopes," J. Global Optim., **29**, pp. 125–155.